Capillary evaporation of the ionic liquid [EMIM][BF_4] in nanoscale solvophobic confinement

Gourav Shrivastav, Richard C. Remsing, and Hemant K. Kashyap

Citation: The Journal of Chemical Physics **148**, 193810 (2018);
View online: https://doi.org/10.1063/1.5010259
View Table of Contents: http://aip.scitation.org/toc/jcp/148/19
Published by the American Institute of Physics

Capillary evaporation of the ionic liquid [EMIM][BF_4] in nanoscale solvophobic confinement

Gourav Shrivastav,[1] Richard C. Remsing,[2,a)] and Hemant K. Kashyap[1,a)]
[1]*Department of Chemistry, Indian Institute of Technology Delhi, Hauz Khas, New Delhi 110016, India*
[2]*Institute for Computational Molecular Science and Department of Chemistry, Temple University, Philadelphia, Pennsylvania 19122, USA*

(Received 24 October 2017; accepted 12 January 2018; published online 29 January 2018)

Solvent density fluctuations play a crucial role in liquid-vapor transitions in solvophobic confinement and can also be important for understanding solvation of polar and apolar solutes. In the case of ionic liquids (ILs), density fluctuations can be used to understand important processes in the context of nanoscale aggregation and colloidal self-assemblies. In this article, we explore the nature of density fluctuations associated with capillary evaporation of the IL 1-ethyl-3-methylimidazolium tetrafluoroborate ([EMIM][BF_4]) in the confined region of model solvophobic nanoscale sheets by using molecular dynamics simulations combined with non-Boltzmann sampling techniques. We demonstrate that density fluctuations of the confined IL play an important role in capillary evaporation, suggesting analogies to dewetting transitions involving water. Significant changes in the interfacial structure of the IL are also detailed and suggested to underlie a non-classical (non-parabolic) dependence of the free energy barrier to evaporation on the degree of confinement. *Published by AIP Publishing.* https://doi.org/10.1063/1.5010259

I. INTRODUCTION

Ionic liquids (ILs) are a class of fused organic salts that are in the liquid state at ambient conditions. The properties of ILs can be tuned through judicious selection of the constituent cations and anions. Because of their negligible vapor pressure, good ionic conductivity, high thermal stability, and broad window of electrochemical stability, ILs have attracted much attention in basic science and industrial applications.[1–5] The promising role of ILs as solvents is ubiquitous;[6,7] they have been applied in catalysis,[1,2,5] as media for enzymatic reactions,[8,9] as electrolytes,[4,10] in synthesis,[1,2,5,11,12] and in separation science.[3,13,14] More recently, ILs have garnered attention for controlling the mechanism of nanoscale assembly.[15,16] Nanoscale solutes, such as graphene sheets, form stable dispersions in ILs, and these dispersions have been used to improve the characteristics of electrical double-layer capacitors (EDLCs).[17–19] Gels of these dispersions have also found application in dye-sensitized solar cells,[20,21] further illustrating the potential of ILs to improve sustainability.

The extended interfaces formed when ILs contact nanoscale solutes and confining surfaces manifest structures and dynamics that are significantly different than those of the bulk IL. Understanding the impact of such interfaces on the properties of ILs and their solutions can guide the development of IL-based technologies, including catalysis, ionogels, supercapacitors, and lubrication. Recently, atomic force microscopy,[22,23] surface force measurements,[24–26] and X-ray reflectivity[27] have been used to study the layering of ILs at extended surfaces, and molecular simulations have provided molecular-scale insights into the structural ordering of ILs at these interfaces.[28–31] In addition, the dynamics of ILs are typically slowed near surfaces, and dynamics are further slowed as the degree of confinement is increased.[26,32–37]

In many applications, self-assembly and EDLCs in particular, *solvophobic effects*, whereby solvent-induced forces drive the assembly of solutes, may play an essential role. In water, solvophobic effects are well-known (termed hydrophobic effects in this case), and they play a key role in a vast array of processes, including protein folding and self-assembly.[38,39] The physical origin of solvophobicity is general, arising from an interplay among solvent density fluctuations, interface formation, and solute-solvent attractions. Thus, solvophobic effects are not specific to a particular solvent although the details will vary and depend on the specific nature of the solvent-solvent interactions.[39,40]

ILs have been suggested to display significant solvophobic effects that can be used to facilitate the formation of self-assembled structures, such as micelles, vesicles, bilayers, and nanoparticle organizations,[16,41] similar to water. Previous work has even suggested that solvophobic effects in ILs can be more significant than those in some molecular organic solvents.[42] Although the structure of ILs in confinement and at interfaces is now becoming increasingly understood,[22–37] our understanding of the thermodynamics of solvophobicity in ILs is limited, and further investigation is needed to inform the development of applications that involve ILs at extended interfaces.

In this work, we use molecular simulations to characterize the thermodynamics of capillary evaporation of the IL 1-ethyl-3-methylimidazolium tetrafluoroborate ([EMIM][BF_4]) when confined between model solvophobic surfaces, where the specific IL was chosen as a representative of the broader

a)Authors to whom correspondence should be addressed: rremsing@temple.edu and hkashyap@chemistry.iitd.ac.in

class of alkylimidazolium-based ILs with nearly spherical anions because it is readily available, its properties are well-documented throughout the literature, and it is relevant for both assembly and EDLC applications.[1,43–50] This process of liquid evaporation in solvophobic confinement could play a role in determining relevant pore sizes for electrochemical devices[18,51–53] and is crucial in assembly processes.[15,38–40] For example, the free energy of assembling two graphene sheets in 1-alkyl-3-methylimidazolium hexafluorophosphate ($[C_nMIM][PF_6]$) ILs was found to be inhibited by large free energy barriers, which are not present in aqueous media due to capillary evaporation (or dewetting) of water between the sheets that drives aggregation.[54]

Dewetting transitions are a direct consequence of solvophobic effects involving extended interfaces.[38,39] Relatively large solvophobic surfaces may induce the formation of soft, liquid-vapor-like interfaces in their vicinity, in the sense that interfacial fluctuations are significant and the interface is easily deformed.[38,39,55,56] When the separation between two such surfaces is less than or equal to some critical distance, d_c, the liquid state becomes metastable with respect to the vapor, and a transition to the vapor phase is accessible. In general, for a liquid confined between two rigid, square parallel plates of size $L \times L$ at a separation of d, the free energy of the corresponding vapor is given by[57]

$$\Omega_v = -p_v L^2 d + 2\gamma_{vs} L^2 + 2\gamma_{ls} L^2 + 4\gamma_{vl} L d, \tag{1}$$

where p_v is the pressure of the vapor, and γ_{ls}, γ_{vs}, and γ_{vl} are the liquid-solid, vapor-solid, and vapor-liquid interfacial tensions, respectively. In conjunction with the free energy of the liquid phase, this expression can be used to estimate the critical distance, which is given by[57]

$$\frac{1}{d_c} = -\frac{(p_l - p_v)}{2\gamma_{vl}\cos\theta} - \frac{2}{L\cos\theta}, \tag{2}$$

where p_l is the pressure of the bulk liquid and θ is the contact angle.

The nature of dewetting transitions involves an interplay of interface formation and density fluctuations in the liquid. Previous work has explored the role of density fluctuations in the dewetting of hydrophobic sheets by water.[58,59] For such dewetting, a non-classical mechanism was suggested wherein vapor bubbles, stabilized by enhanced density fluctuations at the water-plate interface, are formed prior to transitioning into a vapor tube that spans from plate to plate.[58,60] Consequently, the free energy barrier to capillary evaporation can be lower than expected from classical theories.[58] Capillary evaporation in solvated electrolytes has also been investigated,[61] and here we demonstrate that such transitions can occur and may be important in concentrated electrolytes.

The wetting of graphene by water and ILs can be further contrasted by examining contact angles. For water on the surface of graphene,[62] the contact angle is found to be in the range of 95°-100°, which increases to 120° for hydrophobic sheets.[58] Contrary to this, Burt *et al.* used coarse-grained models to suggest that $[EMIM][BF_4]$ completely wets graphene sheets.[63] It was further demonstrated there that modified pseudo-graphene surfaces, with a Lennard-Jones (LJ) well-depth (ϵ) of 0.15 kJ/mol (smaller than the 0.23 kJ/mol for graphene), have IL contact angles of ≈40°.[63] Interestingly, on further reduction of ϵ, the contact angle gradually increases up to ≈146°,[63] illustrating that the general solvophobicity of the model graphene-like surfaces can be tuned through their interactions with the ILs.

Here, we characterize the dewetting thermodynamics of IL $[EMIM][BF_4]$ in nanoscale confinement between *model* solvophobic surfaces, whose interactions with the IL are chosen to yield a contact angle of approximately 140°.[63] We find that enhanced density fluctuations at the surface of solvophobic plates can reduce free energy barriers, similar to previous investigations involving water. Our findings additionally suggest that confinement-induced changes in interfacial structure can significantly impact the free energy barrier to capillary evaporation. The understanding of IL dewetting thermodynamics provided by this work is expected to aid in the development of many IL-based technologies, including lubricants, dispersion media for nanoparticles and colloids, EDLCs, and non-aqueous biological and other self-assembly processes.

II. SIMULATION METHODOLOGY

Capillary evaporation between rigid, nanoscale sheets is studied using molecular dynamics (MD) simulations with GROMACS combined with non-Boltzmann sampling techniques at T = 310 K.[64] Simulation cells consisted of 1500 ion pairs in a 6.5 nm × 14.5 nm × 6.5 nm orthogonal box. A pair of 3 nm × 3 nm sheets, consisting of 1170 atoms arranged on a hexagonal lattice, was kept fixed in the bulk of the IL and aligned with the xy-plane. The LJ interaction parameters for the sheet atoms were adapted from Ref. 58. For the interactions of graphene with ionic liquids, it has been shown that the LJ parameters are sufficient enough to capture the short and long range behavior.[54] The value of the LJ well-depth used here (ϵ = 0.022 kJ/mol) is considerably lower than the value for graphene sheets (0.23 kJ/mol), in order to ensure a significantly solvophobic surface model.[54] Because we are concerned only with the effects of solvophobicity and are employing a model surface, not a physical model of graphene, for example, polarization effects are not considered. The parameters for $[EMIM][BF_4]$ were taken from OPLS-AA/AMBER force-fields proposed by Lopes and Pádua (CL&P),[65–69] using Lorentz-Berthelot combination rules for the off-diagonal elements of the LJ potentials. To mimic a constant pressure ensemble, a liquid-vapor interface was created [see Figs. 1(a) and 1(b)]. Following previous work,[58] a neutral repulsive wall consisting of 676 atoms arranged on a square lattice was used to keep the system from drifting in the direction perpendicular to the liquid-vapor interface. The interaction between the atoms of the repulsive wall and the atoms of the IL was given by a LJ potential with fixed parameters, σ = 0.3855 nm and $\epsilon = 0.6941 \times 10^{-4}$ kJ/mol. For each simulation, a standard three-dimensional periodic boundary condition was applied. Equations of motion were integrated using the leap-frog algorithm with a time step of 1 fs. A cutoff radius of 1.2 nm was used for the evaluation of short-ranged interactions. Electrostatic interactions were evaluated using the particle mesh Ewald summation technique with sixth order

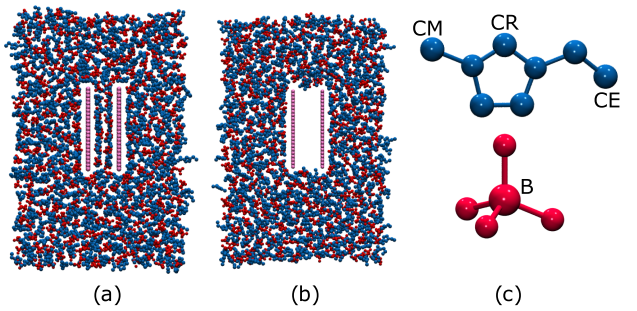

FIG. 1. Representative simulation snapshots for the (a) liquid and (b) vapor phase in the confinement of nanoscale solvophobic square sheets. (c) Structure of [EMIM][BF_4] used in the study. Only heavy atoms are shown for clarity.

interpolation and a Fourier grid spacing of 0.08 nm. The temperature was maintained using the Nosé-Hoover thermostat with the damping relaxation constant of 0.2 ps. Each system was equilibrated for 8 ns using standard MD simulations before performing the non-Boltzmann sampling necessary to probe dewetting transitions.

Capillary evaporation of the IL was quantified by computing the probability $P_v(N)$ of observing N heavy atoms in the volume v between the two plates for varying inter-plate distances, d. The order parameter N was sampled using the indirect umbrella sampling (INDUS) approach, which applies a biasing potential to the continuous variable $\tilde{N}$, which is obtained by coarse-graining the discrete variable N.[55,70] To sample N adequately, we employ the harmonic biasing potential $U(\tilde{N}) = \kappa(\tilde{N} - \tilde{N}^*)^2/2$, with $\tilde{N}^*$ varied over the range of −10 to 600 with a spacing of 10. The value of the harmonic spring constant κ was 0.3 kJ/mol for all biased simulations. The INDUS potential was applied to only the heavy atoms, not hydrogens, of both cations and anions. Each biased simulation was 50 ns in duration, and the free energies $\Delta G(N) = -\beta^{-1} \ln P_v(N)$ were computed from the umbrella sampling simulations using the weighted histogram analysis method (WHAM),[71] with errors estimated through block averaging using 5 blocks of the last 10 ns trajectory, where $\beta = 1/k_B T$ and k_B is Boltzmann's constant.

III. RESULTS AND DISCUSSION

The free energies $\Delta G(N)$, shown in Fig. 2, are consistent with expectations for capillary evaporation of a solvent in solvophobic confinement near liquid-vapor coexistence. Fluctuations in the liquid basin display significantly non-Gaussian, fat tails at low N (see the inset of Fig. 2). These enhanced fluctuations arise from the proximity of the liquid phase to coexistence with its vapor and indicate nucleation of a vapor cavity within the liquid. This additionally suggests that the formation of cavities is stabilized at the surface of the plates, as observed previously for water.[55,58,60,72] As N is further decreased, a free energy barrier is encountered. The free energy landscape on the low N side of this barrier is consistent with the radial growth of an approximately cylindrical vapor tube that spans the inter-plate distance. This suggests that the general thermodynamic driving forces underlying capillary evaporation of ILs are analogous to those in water,[58,60] although, as detailed

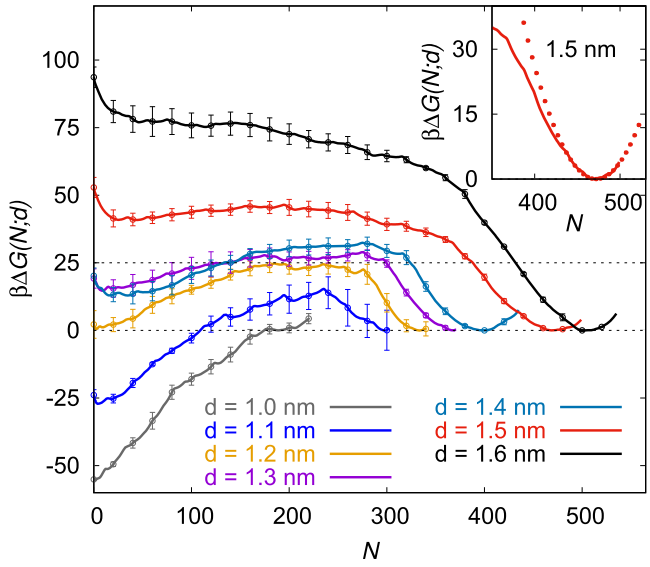

FIG. 2. Simulated free energy profiles as a function of the number of heavy atoms in the confinement of sheets. Here, $\beta = 1/k_B T$ where k_B is the Boltzmann constant and T is the temperature. The inset shows a parabolic fit (points) to the liquid basin of the 1.5 nm system as a representative example illustrating the deviation from Gaussian statistics as N is decreased. Error bars indicate one standard deviation.

below, differences remain due to the structural ordering of the IL in confinement.

At high d-values, a stable liquid basin is observed, and at d = 1.6 nm, only the liquid state is stable; there is no well-defined vapor basin. As d is decreased, a metastable vapor basin develops at low N, separated from the liquid state by a significant free energy barrier. Coexistence of the liquid and vapor phases occur near $d_c \approx 1.2$ nm, with a free energy barrier of $\approx 25\ k_B T$ separating the two states.

In contrast, for plates of a similar size and attractiveness in water, $d_c \approx 1.4$ nm, and the corresponding free energy barrier at d_c of roughly $18 k_B T$.[73] This suggests that solvophobic effects are relatively weaker in ILs, consistent with previous suggestions.[15] From Eq. (2), the lower d_c of the IL can be ascribed to its lower surface tension[74,75] and contact angle. Below d_c, a stable vapor phase and metastable liquid phase are found. Even at d = 1.1 nm, the stable vapor state is separated from its metastable liquid state by a considerable barrier of $\approx 15\ k_B T$. Finally, for $d \leq 1.0$ nm, the liquid phase becomes unstable with respect to the vapor.

In recent work, Gogotsi and co-workers showed that for slit widths <0.7 nm and zero applied potential, ions did not wet a carbon electrode.[52] Kondrat *et al.* have also found similar behavior by reducing the ion-wall interaction strength.[18] Although the reported separations are slightly lower than those observed in our study, this difference in the critical distance may be attributed to different ion-wall interactions captured by the contact angle in Eq. (2). Stronger surface-IL interactions (lower θ) are expected to decrease the critical distance d_c. This can be further supported by the fact that for graphene sheets in ILs, aggregation of sheets occurs below 0.6 nm.[54] At such a small separation, the ions are unable to penetrate the inter-plate space due to excluded volume interactions. This is consistent with the complete wetting of graphene by some ILs.

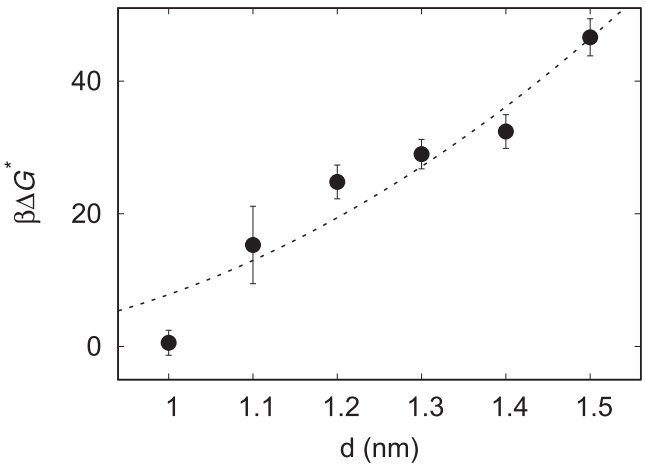

FIG. 3. Free energy barrier as a function of inter-plate distance d. Dashed line shows the best fit to the functional form of Eq. (3). Error bars indicate one standard deviation.

The free energy barrier separating the liquid and vapor basins corresponds to the cost of forming a plate-spanning vapor tube. Because this barrier is due to the formation of an extended interface, it is largely enthalpic in nature. In water and simple fluids, this free energy barrier, ΔG^*, closely follows macroscopic theory, which predicts that ΔG^* scales quadratically with d,[58]

$$\Delta G^*(d) \approx -\frac{2\pi\beta\gamma_{vl}}{\cos\theta}\left[\frac{\tilde{d}^2}{4} + \tilde{d}\left(\frac{\lambda}{\gamma_{vl}}\right) + \left(\frac{\lambda}{\gamma_{vl}}\right)^2\right], \qquad (3)$$

where $\tilde{d} \equiv d - d_p$ is the available distance between the sheets, such that d_p is roughly the size of a plate atom, and λ is the line tension. In contrast, the d-dependence of ΔG^* is more complex in the IL. As shown in Fig. 3, the simulated ΔG^* are not fit well by the functional form of Eq. (3), in contrast to water,[58] and systematic deviations from the macroscopic form are observed. We attribute these deviations to structural changes that the IL undergoes at the surface as d is varied.

Figure 4 shows the number density distribution of the terminal carbon of the methyl group (CM) of the cation, the terminal carbon of the ethyl group (CE) of the cation, the center carbon of the ring (CR), and the boron (B) of the anion, evaluated within the liquid basin of the IL confined between the model solvophobic surfaces. For all separations, a dense layering of terminal carbon atoms is clearly visible in close proximity to the sheet surface. At d = 1.0 nm, only a single layer is present which is observed through the single peak in the CR density. The non-overlapping peak behavior of CR with CM and CE is consistent with non-parallel orientations, where the CM or CE point toward the surface with the cation ring (CR) toward the center of the confined space.

At d = 1.1 nm, Fig. 4(b), two layers are observed. The peak positions of the CM, CE, and CR densities overlap, indicating that the cations are oriented parallel to the plate surface. In addition, the peak in CR density at the center of the confined space [Fig. 4(b)] suggests that some of the cations adopt an orientation with an ethyl group interacting with one sheet and a methyl group with the other. Two peaks corresponding to anions are also present in the proximity of the cation ring, supporting this two-layer picture.

As the inter-plate distance is expanded to d = 1.3 nm, Fig. 4(c), the orientation of the cations changes and a change in the curvature of ΔG^* is observed. There are again two layers present, but the cation rings are no longer parallel to the plate surface. The alkyl chains point toward the plate surfaces and the cation rings are located further from the surface.

At d = 1.5 nm [Fig. 4(d)], the interfacial structure changes again with a concomitant deviation in ΔG^*. The densities of alkyl groups (CM, CE) and anions (B) show three layers, while the cation ring (CR) densities have five peaks. At the surface of the plates, the CR, CM, and CE densities overlap, indicating that the cations are oriented parallel to the surface. The CR peak at the center of the confined region also overlaps with peaks in the CM and CE densities, suggesting a parallel arrangement in this region as well. Cation rings are additionally found in the region between these two peaks, where a peak in the CR density is observed at a minimum in the other densities, and the cations point their alkyl groups toward the plates. These observations are consistent with previous results obtained for layering of an IL between graphene sheets.[31]

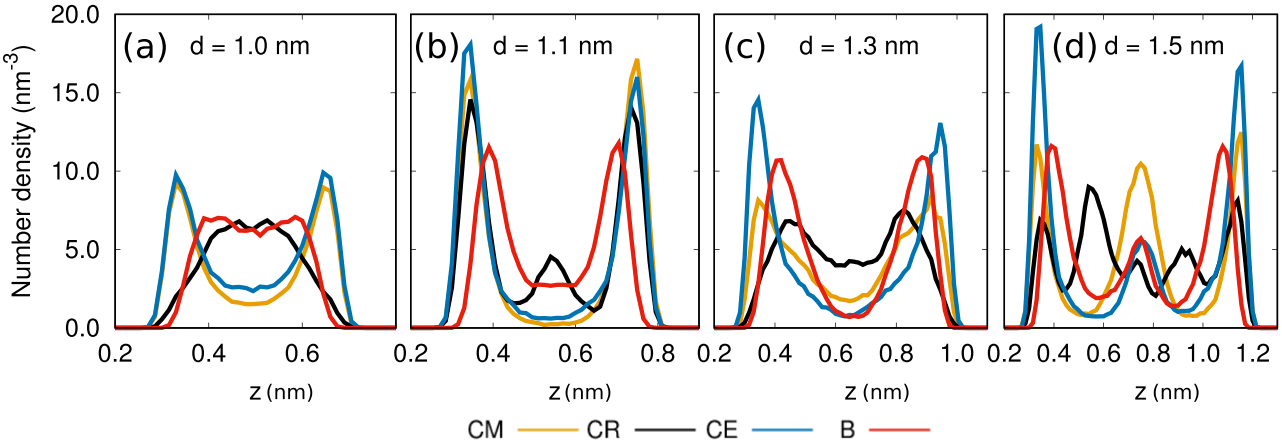

FIG. 4. Number density distribution of atomic sites for [EMIM][BF_4] between solvophobic/ionophobic rigid, nanoscale sheets at several values of the inter-plate separation d. The densities are computed from configurations with N corresponding to the liquid basin.

The structural changes of the IL induced by the varying degrees of confinement are suggested to underlie the changes observed in the free energy barriers as a function of d, as well as the non-linear changes in the liquid density with d apparent in Fig. 2. Changes in the orientational ordering of cation rings alter the manner in which the IL wets the sheets, changing the values of $\cos\theta$ and λ, and consequently lead to deviations in ΔG^* from a single parabolic form, Eq. (3). Instead, these structural changes may lead to a piecewise parabolic scaling of ΔG^* on d, for example, with each individual scaling specific to distinct interfacial wetting structures. Structural changes have also recently been suggested to underlie changes in the kinetics of capillary evaporation of water in hydrophobic confinement.[76]

Due to the diversity of structures in the vast array of ILs, we do not think there will be a universal form for the scaling of the free energy barriers. However, we do expect that the qualitative trends observed here will be observed from similar alkylimidazolium-based ILs with approximately spherical anions, e.g., alkylimidazolium halides, tetrafluoroborates, and hexafluorophosphates. More detailed studies beyond the scope of the current work, which systematically quantify the relationship between interfacial structure, contact angles, and line tensions, are needed to characterize the detailed scaling behavior of $\Delta G^*(d)$ in ILs.

IV. CONCLUSIONS

To conclude, we have shown that [EMIM][BF_4] exhibits weaker solvophobic effects than water, which can be explained by considering the relevant thermodynamic parameters, such as the contact angle and surface tension. Moreover, our results suggest that free energy barriers to dewetting in ILs and other complex liquids may depend sensitively on confinement-induced structural changes as layers of the liquid are extruded from the confined space. It is illustrated that even with the weakly interacting surfaces, spontaneous evaporation occurs when there is only a single layer of ions present in confinement, $d < 1.2$ nm. Inter-plate separations of 1.2–1.4 nm, which have ample space to accommodate two layers of ions, exhibit a stable liquid phase with a metastable vapor phase.

Understanding these thermodynamic aspects of solvophobicity in ILs may aid in the improvement and extension of many IL-based applications. For example, dewetting transitions can significantly impact the kinetics of assembly,[77–79] and probing the underlying free energy landscape can aid the interpretation and design of assembly processes. Understanding capillary evaporation in ILs should also shed light on relevant pore sizes in nanoporous carbon electrodes. In particular, one can envision combining capillary evaporation in nanopores with electrowetting to enhance capacitance. Solvophobic nanopores may be dry without an applied potential. Under an applied potential, the contact angle will decrease, and the IL will increasingly wet the surface, which leads to a concomitant decrease in the critical distance for evaporation [Eq. (2)].[63,80–82] We conclude by noting that small changes in the flexibility of confining plates, not included here, can significantly impact the thermodynamics and kinetics of capillary evaporation[60] and can be used to further tune solvophobic effects in IL-based systems.

ACKNOWLEDGMENTS

H.K.K. sincerely thanks Professor Ranjit Biswas, Professor Claudio J. Margulis, and Professor Edward W. Castner, Jr. for support and encouragement. G.S. thanks the CSIR, India for fellowship. We thank the IIT Delhi HPC facility for computational resources. This work is financially supported by the Department of Science and Technology (DST), India, through FIST and a grant awarded to H.K.K. (Grant No. SB/FT/CS-124/2014). R.C.R. was supported as part of the Center for the Computational Design of Functional Layered Materials, an Energy Frontier Research Center funded by the U.S. DOE, Office of Science, Basic Energy Sciences under Award No. DE-SC0012575. R.C.R. also acknowledges an APS-IUSSTF Physics Post-doc Visitation Program award.

[1] T. Welton, Chem. Rev. **99**, 2071 (1999).
[2] E. W. Castner, Jr., C. J. Margulis, M. Maroncelli, and J. F. Wishart, Annu. Rev. Phys. Chem. **62**, 85 (2011).
[3] J. G. Huddleston, H. D. Willauer, R. P. Swatloski, A. E. Visser, and R. D. Rogers, Chem. Commun. **0**, 1765 (1998).
[4] M. Galinski, A. Lewandowski, and I. Stepniak, Electrochim. Acta **51**, 5567 (2006).
[5] J. P. Hallett and T. Welton, Chem. Rev. **111**, 3508 (2011).
[6] J. G. Huddleston, A. E. Visser, W. M. Reichert, H. D. Willauer, G. A. Broker, and R. D. Rogers, Green Chem. **3**, 156 (2001).
[7] J. F. Brennecke and E. J. Maginn, AIChE J. **47**, 2384 (2001).
[8] M. Moniruzzaman, K. Nakashima, N. Kamiya, and M. Goto, Biochem. Eng. J. **48**, 295 (2010).
[9] V. W. Jaeger and J. Pfaendtner, ACS Chem. Biol. **8**, 1179 (2013).
[10] M. D. Bennett and D. J. Leo, Sens. Actuators, A **115**, 79 (2004).
[11] M. Antonietti, D. Kuang, B. Smarsly, and Y. Zhou, Angew. Chem., Int. Ed. **43**, 4988 (2004).
[12] F. Endres, Chem. Phys. Chem. **3**, 144 (2002).
[13] D. A. Fort, R. C. Remsing, R. P. Swatloski, P. Moyna, G. Moyna, and R. D. Rogers, Green Chem. **9**, 63 (2007).
[14] D. Camper, J. E. Bara, D. L. Gin, and R. D. Noble, Ind. Eng. Chem. Res. **47**, 8496 (2008).
[15] T. L. Greaves and C. J. Drummond, Chem. Soc. Rev. **42**, 1096 (2013).
[16] Z. He and P. Alexandridis, Phys. Chem. Chem. Phys. **17**, 18238 (2015).
[17] P. Wu, J. Huang, V. Meunier, B. G. Sumpter, and R. Qiao, ACS Nano **5**, 9044 (2011).
[18] S. Kondrat, P. Wu, R. Qiao, and A. A. Kornyshev, Nat. Mater. **13**, 387 (2014).
[19] S. Kondrat and A. A. Kornyshev, Nanoscale Horiz. **1**, 45 (2016).
[20] R. Kawano, H. Matsui, C. Matsuyama, A. Sato, M. B. H. Susan, N. Tanabe, and M. Watanabe, J. Photochem. Photobiol., A **164**, 87 (2004).
[21] M. Gorlov and L. Kloo, Dalton Trans. **0**, 2655 (2008).
[22] R. Atkin and G. G. Warr, J. Phys. Chem. C **111**, 5162 (2007).
[23] R. Hayes, S. Z. El Abedin, and R. Atkin, J. Phys. Chem. B **113**, 7049 (2009).
[24] S. Perkin, T. Albrecht, and J. Klein, Phys. Chem. Chem. Phys. **12**, 1243 (2009).
[25] S. Perkin, L. Crowhurst, H. Niedermeyer, T. Welton, A. M. Smith, and N. N. Gosvami, Chem. Commun. **47**, 6572 (2011).
[26] S. Perkin, Phys. Chem. Chem. Phys. **14**, 5052 (2012).
[27] M. Mezger, S. Schramm, H. Schröder, H. Reichert, M. Deutsch, E. J. De Souza, J. S. Okasinski, B. M. Ocko, V. Honkimäki, and H. Dosch, J. Chem. Phys. **131**, 094701 (2009).
[28] M. V. Fedorov and A. A. Kornyshev, J. Phys. Chem. B **112**, 11868 (2008).
[29] S. Maolin, Z. Fuchun, W. Guozhong, F. Haiping, W. Chunlei, C. Shimou, Z. Yi, and H. Jun, J. Chem. Phys. **128**, 134504 (2008).
[30] M. V. Fedorov, N. Georgi, and A. A. Kornyshev, Electrochem. Commun. **12**, 296 (2010).
[31] M. Alibalazadeh and M. Foroutan, J. Mol. Model. **21**, 168 (2015).

[32]K. Ueno, M. Kasuya, M. Watanabe, M. Mizukami, and K. Kurihara, Phys. Chem. Chem. Phys. **12**, 4066 (2010).
[33]B. Coasne, L. Viau, and A. Vioux, J. Phys. Chem. Lett. **2**, 1150 (2011).
[34]S. Li, K. S. Han, G. Feng, E. W. Hagaman, L. Vlcek, and P. T. Cummings, Langmuir **29**, 9744 (2013).
[35]K. S. Han, X. Wang, S. Dai, and E. W. Hagaman, J. Phys. Chem. C **117**, 15754 (2013).
[36]G. Ori, F. Villemot, L. Viau, A. Vioux, and B. Coasne, Mol. Phys. **112**, 1350 (2014).
[37]S. Zhang, J. Zhang, Y. Zhang, and Y. Deng, Chem. Rev. **117**, 6755 (2016).
[38]K. Lum, D. Chandler, and J. D. Weeks, J. Phys. Chem. B **103**, 4570 (1999).
[39]D. Chandler, Nature **437**, 640 (2005).
[40]R. C. Remsing and J. D. Weeks, J. Chem. Phys. B **117**, 15479 (2013).
[41]T. L. Greaves and C. J. Drummond, Chem. Rev. **108**, 206 (2008).
[42]I. Sedov and B. Solomonov, Fluid Phase Equilib. **425**, 9 (2016).
[43]S. A. Katsyuba, P. J. Dyson, E. E. Vandyukova, A. V. Chernova, and A. Vidiš, Helv. Chim. Acta **87**, 2556 (2004).
[44]N. E. Heimer, R. E. Del Sesto, Z. Meng, J. S. Wilkes, and W. R. Carper, J. Mol. Liq. **124**, 84 (2006).
[45]H. Valencia, M. Kohyama, S. Tanaka, and H. Matsumoto, Phys. Rev. B **78**, 205402 (2008).
[46]D. Han and K. H. Row, Molecules **15**, 2405 (2010).
[47]J. Zheng, S. S. Moganty, P. C. Goonetilleke, R. E. Baltus, and D. Roy, J. Phys. Chem. C **115**, 7527 (2011).
[48]M. J. Shiddiky and A. A. Torriero, Biosens. Bioelectron. **26**, 1775 (2011).
[49]J. B. Haskins, W. R. Bennett, J. J. Wu, D. M. Hernández, O. Borodin, J. D. Monk, C. W. Bauschlicher, Jr., and J. W. Lawson, J. Phys. Chem. B **118**, 11295 (2014).
[50]A. Boruń, C. Fernandez, and A. Bald, Int. J. Electrochem. Sci. **10**, 2120 (2015).
[51]C. Largeot, C. Portet, J. Chmiola, P.-L. Taberna, Y. Gogotsi, and P. Simon, J. Am. Chem. Soc. **130**, 2730 (2008).
[52]J. Vatamanu, Z. Hu, D. Bedrov, C. Perez, and Y. Gogotsi, J. Phys. Chem. Lett. **4**, 2829 (2013).
[53]C. Merletm, C. Pean, B. Rotenberg, P. Madden, B. Daffos, P.-L. Taberna, P. Simon, and M. Salanne, Nat. Commun. **4**, 2701 (2013).
[54]Y. Zhao and Z. Hu, J. Phys. Chem. B **117**, 10540 (2013).
[55]A. J. Patel, P. Varilly, and D. Chandler, J. Chem. Phys. B **114**, 1632 (2010).
[56]A. P. Willard and D. Chandler, J. Chem. Phys. **141**, 18C519 (2014).
[57]Y. E. Altabet and P. G. Debenedetti, J. Chem. Phys. **141**, 18C531 (2014).
[58]R. C. Remsing, E. Xi, S. Vembanur, S. Sharma, P. G. Debenedetti, S. Garde, and A. J. Patel, Proc. Natl. Acad. Sci. U. S. A. **112**, 8181 (2015).
[59]R. Evans and N. B. Wilding, Phys. Rev. Lett. **115**, 016103 (2015).
[60]Y. E. Altabet, A. Haji-Akbari, and P. G. Debenedetti, Proc. Natl. Acad. Sci. U. S. A. **114**, E2548 (2017).
[61]S. Buyukdagli, M. Manghi, and J. Palmeri, Phys. Rev. Lett. **105**, 158103 (2010).
[62]F. Taherian, V. Marcon, N. F. A. van der Vegt, and F. Leroy, Langmuir **29**, 1457 (2013).
[63]R. Burt, G. Birkett, M. Salanne, and X. S. Zhao, J. Phys. Chem. C **120**, 15244 (2016).
[64]D. V. S. Spoel, E. Lindahl, B. Hess, G. Groenhof, A. E. Mark, and H. J. C. Berendsen, J. Comput. Chem. **26**, 1701 (2005).
[65]W. L. Jorgensen, J. D. Madura, and C. J. Swenson, J. Am. Chem. Soc. **106**, 6638 (1984).
[66]G. Kaminski and W. L. Jorgensen, J. Phys. Chem. **100**, 18010 (1996).
[67]R. C. Rizzo and W. L. Jorgensen, J. Am. Chem. Soc. **121**, 4827 (1999).
[68]M. L. P. Price, D. Ostrovsky, and W. L. Jorgensen, J. Comput. Chem. **22**, 1340 (2001).
[69]J. N. C. Lopes, J. Deschamps, and A. A. H. Pádua, J. Phys. Chem. B **108**, 2038 (2004).
[70]A. J. Patel, P. Varilly, D. Chandler, and S. Garde, J. Stat. Phys. **145**, 265 (2011).
[71]S. Kumar, J. M. Rosenberg, D. Bouzida, R. H. Swendsen, and P. A. Kollman, J. Comput. Chem. **13**, 1011 (1992).
[72]K. Lum and A. Luzar, Phys. Rev. E **56**, R6283 (1997).
[73]S. Sharma and P. G. Debenedetti, J. Chem. Phys. B **116**, 13282 (2012).
[74]G. Law and P. R. Watson, Langmuir **17**, 6138 (2001).
[75]M. Tariq, M. G. Freire, B. Saramago, J. A. P. Coutinho, J. N. C. Lopes, and L. P. N. Rebelo, Chem. Soc. Rev. **41**, 829 (2012).
[76]Y. E. Altabet and P. G. Debenedetti, J. Chem. Phys. **147**, 241102 (2017).
[77]J. Mondal, J. A. Morrone, and B. J. Berne, Proc. Natl. Acad. Sci. U. S. A. **110**, 13277 (2013).
[78]J. Li, J. A. Morrone, and B. J. Berne, J. Phys. Chem. B **116**, 11537 (2012).
[79]P. Setny, R. Baron, P. Michael Kekenes-Huskey, J. A. McCammon, and J. Dzubiella, Proc. Natl. Acad. Sci. U. S. A. **110**, 1197 (2013).
[80]F. Taherian, F. Leroy, L.-O. Heim, E. Bonaccurso, and N. F. A. van der Vegt, Langmuir **32**, 140 (2016).
[81]S. Millefiorini, A. H. Tkaczyk, R. Sedev, J. Efthimiadis, and J. Ralston, J. Am. Chem. Soc. **128**, 3098 (2006).
[82]J. M. Black, G. Feng, P. F. Fulvio, P. C. Hillesheim, S. Dai, Y. Gogotsi, P. T. Cummings, S. V. Kalinin, and N. Balke, Adv. Energy Mater. **4**, 1300683 (2014).